

# Experimental study on seismic performance of mechanical/electrical equipment with vibration isolation systems

S.J. Wang, Y.H. Yang, C.Y. Yang, F.R. Lin, J.S. Hwang & K.C. Chang

National Center for Research on Earthquake Engineering, Taipei, Taiwan..

**ABSTRACT:** In this study, a prototype diesel generator equipped with the vibration isolation systems consisting of restrained isolators only (denoted as I/ system) and restrained isolators plus additional snubbers (denoted as I/R system) are dynamically tested. The test results show that the incorporation of snubbers as additional restraints can prevent the restrained isolators from plastic behavior and severe damage. Besides, the acceleration performance of I/R system, in general, is not inferior to that of I/ system. Comparing the test results to the static design demands specified in ASCE 7-10, it is found that the recommended value for the component amplification factor could represent the horizontal acceleration amplification phenomenon of the generator equipped with I/R system; however, the seismic force demands for static design of I/R system might not be appropriate and conservative enough.

## 1 INTRODUCTION

To reduce the vibration induced by regular operation of Mechanical and Electrical (M/E) equipment transmitting to building structures, different types of isolation devices are accommodated for vibration reduction. Commonly used spring isolators for M/E equipment in engineering practice are open, housed, and restrained isolators. The current practical design of spring isolators simply considers the operating weight and frequency of the M/E equipment above while the seismic resistant capability is rarely concerned. Some experiences and lessons from past earthquakes reveal that the implementation of spring isolators may make the M/E equipment above much more seismically vulnerable (EPRI 1991, 1996, FEMA 2007, 2011 and Miranda 2010). So far, there are relatively few experimental researches regarding the seismic resistant capability of spring isolators (Chen 2009 and Lam 1985). Fathali and Filiatrault (2007a and b) examined the dynamic characteristics of an ASHRAE-type (formerly the American Society of Heating, Refrigerating and Air conditioning Engineers) isolation/restraint system consisting of coil springs and built-in elastomeric snubbers by conducting shaking table tests for a centrifugal liquid chiller mounted on such system. It was indicated that the isolation/restraint system could reveal an adorable seismic performance if the snubbers were properly designed. For the input motions with peak acceleration (PA) larger than 0.15 g, which was high enough to engage the restraint components, the acceleration amplification factors at the center of mass and the corners of the rigidly mounted chiller decreased with an increase of peak input acceleration.

In this study, a prototype diesel generator is selected as the test specimen, and the seismic performance of the vibration isolation systems composed of restrained isolators only and restrained isolators plus additional snubbers, respectively called “I/ system” and “I/R system”, are experimentally discussed. Based on the shaking table test results of I/R system, the design value of the component amplification factor together with the seismic design forces for vibration isolated components and systems recommended in ASCE 7-10 (ASCE 2010) are further examined.

## 2 SEISMIC SIMULATION TEST

### 2.1 Input acceleration excitations

According to ASCE 7-10 (ASCE 2010) and AC156 (ICC-ES 2010), the horizontal seismic design force for nonstructural components, denoted as  $F_{ph}$  thereafter, is determined by

$$F_{ph} = \frac{0.4a_p S_{DS} W_p}{(R_p/I_p)} \left( 1 + 2 \frac{z}{h} \right) \quad (1)$$

As specified in AC156 (ICC-ES 2010), the design reduction factor ( $R_p/I_p$ ) should be set equal to 1.0 since the inelastic behaviour of the test unit will naturally occur during seismic simulation tests.  $I_p$  does not increase the input motion but does affect the requirement for the test unit.  $a_p=2.5$  and  $a_p=1.0$  are respectively adopted for flexible (flexibly attached) and rigid (rigidly attached) components, which also respectively correspond to the amplified region and the zero period acceleration (ZPA) of the 5% damped horizontal required response spectrum (RRS). Besides, the vertical RRS shall be developed based on two-thirds of the ground-level base horizontal acceleration (*i.e.*,  $z/h$  is taken as 0). Thus, the vertical seismic design force, denoted as  $F_{pv}$  thereafter, is determined by the following equation, which can also meet the minimum design requirement specified in ASCE 7-10 (ASCE 2010)

$$F_{pv} = \frac{2}{3} (0.4S_{DS}W_p) > 0.2S_{DS}W_p \quad (2)$$

The test specimen is assumed to be placed at either the first floor or the roof of a hospital building at different sites. As detailed in Table 1, four RRS-compatible triaxial floor acceleration histories considering different values of  $S_{DS}$  and  $z/h$ , denoted as AC156-1F-1, AC156-1F-2, AC156-1F-3, and AC156-RF thereafter, were generated as triaxial acceleration inputs. Each generated acceleration history was scaled to have different PA values.

## 2.2 Test Scheme I: generator module equipped with restrained isolators only (I/ system)

The decomposition of the restrained isolator (YS-2-2400A25) manufactured by the YS-AIR company is illustrated in Fig. 1 (Harmony Rubber Industry Co. Ltd.). The generator module equipped with the vibration isolation system composed of four restrained isolators (I/ system) were tested in this scheme, as shown in Fig. 2. Load cells, cable-extension displacement sensors, and triaxial accelerometers were installed for dynamic response measurement. Before conducting seismic simulation tests, the triaxial fundamental modal periods of vibration and the equivalent damping ratios of the generator module equipped with I/ system were respectively identified by sine sweep and impulse tests, as summarized in Table 2.

As observed during the tests and from the acceleration response histories, because of instantaneous pounding induced by the air gap existing in the restrained isolators, there exist notable spikes in acceleration responses. The root mean square (RMS) values, rather than the peak values, of the transmission ratios of acceleration response histories measured at different positions (A1 to A4) to triaxial input acceleration histories with different PA scales are presented in Fig. 3. To exclude the flexibility effect of the generator module, A5 and A6 are not discussed in the following. Because rocking motion of the test specimen was observed during the tests and experimentally identified as summarized in Table 2, the acceleration transmission ratios in Z direction are much larger compared to those in X direction. In addition, since rocking motion along longitudinal (X) direction is more severe than that along transverse (Y) direction, the acceleration transmission ratios in Y direction are much greater than those in X direction.

The hysteresis loops of Isolator 2, Isolator 4, and I/ system subjected to 120% triaxial AC156-RF are shown in Fig. 4, from which the evident inelastic behavior in two horizontal directions is observed. Besides, in X or Y direction, the forward and reverse hysteresis loops of a single restrained isolator are not very skew symmetric. It is mainly attributed to rocking motion of the test specimen observed during the tests. Theoretically, the vertical mechanical behavior of the restrained isolators should remain essentially elastic. However, due to the interaction of horizontal and vertical excitations and/or responses, such as the influence arising from plastic flexural deformation of the vertical restraint rods or collision between the vertical restraint nuts and restraint base, the vertical dynamic behavior of the restrained isolators under triaxial excitations observed from Fig. 4 becomes more complicated, but still has a tendency toward elastic behavior.

The tested restrained isolators were not visibly damaged until subjected to 120% triaxial AC156-RF, which is the most rigorous test condition and beyond design level in horizontal directions. The failure modes are fatigue damage of the connection between the vertical restraint rods and top plate together with pull-out failure of the vertical restraint rods, as observed in Fig. 5.

### 2.3 Test Scheme II: generator module equipped with restrained isolators and additional snubbers (I/R system)

A combination of restrained isolators and additional bumpers or snubbers in the vibration isolation system (I/R system) is suggested in ASCE 7-10 (ASCE 2010) for seismic concerns. In this scheme, to compare and further discuss the seismic responses of a generator module respectively equipped with I/ and I/R systems, the same test specimen and vibration isolation system but additionally equipped with four snubbers were tested, as shown in Fig. 2. Manufactured by the YS-AIR company (Harmony Rubber Industry Co. Ltd.), the structure of the snubber (YS-7500EL) is very similar to a hinge device (i.e., a core rod is inserted into a hollow cylinder and is fixed with a bracket at both ends), as shown in Fig. 6. The inside surface of the hollow cylinder and the two inside surfaces of the bracket are coated with rubber. There still exists an average 3 mm thick cylindrical air gap between the core rod and the coated rubber of the inside surface of the hollow cylinder, and between the hollow cylinder and the coated rubber of the two inside surfaces of the bracket. Besides, the installation layout of measurement instrumentations is the same as that for Test Scheme I except additional load cells for triaxial force response capture of four snubbers, as shown in Fig. 2. The system identified characteristics for Test Scheme II are also presented in Table 2.

Because of instantaneous pounding induced by the air gap existing in the restrained isolators and snubbers, some spikes in acceleration responses are still inevitable. The acceleration transmission ratios in Test Scheme II are also presented in Fig. 3. In addition, rocking motion of the test specimen in Test Scheme II was still observed during the tests and also experimentally identified as summarized in Table 2, leading to the same trend in X, Y, and Z directions as Test Scheme I. As observed from Fig. 3, even if there exists additional resistant stiffness contributed by the snubbers, the acceleration response performance of I/R system, in general, is not worse than that of I/ system. It is because that the coated rubber in the snubbers can moderately mitigate the aforementioned pounding effect.

The comparison of hysteresis loops of the restrained isolators and vibration isolation systems in Test Schemes I and II subjected to 120% triaxial AC156-RF are shown in Fig. 4, from which it can be seen that the dynamic behavior of the restrained isolators in Test Scheme II essentially remains elastic. As expected, because of additional restraints provided by the snubbers, the horizontal and vertical displacement responses of the vibration isolation system in Test Scheme II can be significantly reduced compared to those in Test Scheme I. Most importantly, even subjected to the most rigorous test condition and beyond design level like 120% triaxial AC156-RF, the tested restrained isolators and snubbers can remain fully intact.

### 2.4 Discussion on recommended values for component amplification factor and seismic design force in ASCE 7-10

The generator module equipped with different vibration isolation systems discussed in Test Schemes I and II can be rationally regarded as a flexible (flexibly attached) component because the identified fundamental modal frequencies in three directions, as listed in Table 2, are less than 16.7 Hz. Referring to Table 13.6-1 provided in ASCE 7-10 (ASCE 2010), only the latter, the generator module equipped with I/R system, can be categorized as “Vibration Isolated Components and Systems: spring isolated components and systems and vibration isolated floors closely restrained using built-in or separate elastomeric snubbing devices or resilient perimeter stops.” Hence, the values of  $a_p$  and  $R_p$  for static design of I/R system are recommended as 2.5 and 2.0, respectively.

To discuss the applicability of the recommended  $a_p$  value for the generator module equipped with I/R system,  $a_p = 2.5$  is plotted in Fig. 3. In addition, the information of mean ( $\mu$ ) and standard deviation ( $\sigma$ ) is provided in Fig. 3 for better comparison. It can be found that  $a_p = 2.5$  might be capable of representing the horizontal acceleration amplification phenomenon of the generator module equipped with I/R system, especially when the peak input acceleration becomes larger. However, because of the aforementioned rocking effect,  $a_p = 2.5$  is slightly or significantly smaller than most of ( $\mu - \sigma$ ) values in Y and Z directions, respectively. To sum up, the recommended  $a_p$  value in ASCE 7-10 (ASCE 2010) for I/R system might be conservative enough for the horizontal seismic performance concern of the equipment above, but it greatly underestimates the actual vertical response especially when rocking motion occurs.

The horizontal and vertical seismic design forces for I/R system can be respectively determined by using Equations (1) and (2) considering different  $S_{DS}$  and  $z/h$  values specified in Table 1. Substituting  $a_p=2.5$ ,  $R_p=2.0$ ,  $I_p=1.0$ , and  $W_p=5500$  kg into Equations (1) and (2),  $F_{ph}$  and  $F_{pv}$  ( $S_{DS}=0.8$ ) for I/R system at the first floor of a hospital building can be calculated as 21.58 kN and 11.51 kN, respectively. Similarly,  $F_{ph}$  and  $F_{pv}$  ( $S_{DS}=0.6$ ) for I/R system at the roof can be calculated as 48.56 kN and 8.63 kN, respectively. The measured maximum force responses transmitted by I/R system under all the triaxial input acceleration histories excluding 120% triaxial AC156-RF (beyond design level), together with the calculated  $F_{ph}$  and  $F_{pv}$  values, are presented in Fig. 7. In addition, the following information is provided in the figure for further discussion:

1. Indicated in ASCE 7-10 (ASCE 2010), if the nominal clearance (air gap) between the equipment support frame and restraints is greater than 6 mm, the design force shall be taken as  $2F_{ph}$  in horizontal direction (or  $2F_{pv}$  in vertical direction). Even though the air gaps existing in the tested restrained isolators and snubbers are equal to or less than 6 mm, the values of  $2F_{ph}$  and  $2F_{pv}$  are also plotted in Fig. 7.
2. As observed from Fig. 4, the value of  $R_p > 1.0$  might not be very appropriate to represent the actual plastic behavior of I/R system. Therefore, the horizontal seismic design forces without considering the component response modification factor (i.e.,  $R_p = 1.0$ ) are also plotted in Fig. 7.

As observed from the comparison between the measured maximum force responses under 100% acceleration excitations and the corresponding design forces, it can be seen that the test results are significantly beyond the design forces determined by Equations (1) and (2) using the recommended values,  $a_p=2.5$  and  $R_p=2.0$ . It is particularly apparent for the vertical direction, even if the vertical design force has been conservatively determined using two-thirds, rather than half, of the ground-level base horizontal acceleration. Either adopting  $2F_{ph}$  or considering  $R_p=1.0$ , or both aforementioned, might provide a more conservative horizontal seismic design force. Therefore, Equations (1) and (2) might improperly represent and even greatly underestimate the observed actual dynamic behavior of I/R system, which coincide with the conclusion in the previous research (Fathali 2007a).

### 3 CONCLUSION

Some conclusions are made as follows:

1. Because of contact between the vertical restraint rods and restraint base, plastic flexural deformation of the vertical restraint rods, and sliding motion between the top bolt and top plate or between the spring module and restraint base, the restrained isolators reveal nonlinear and complicated mechanical behavior.
2. The failure modes of the restrained isolators are severe fatigue damage of the connection between the vertical restraint rods and top plate together with pull-out failure of the vertical restraint rods. It should be further improved especially when the restrained isolators are used in earthquake-prone areas.
3. It is obvious that, due to the interaction of horizontal and vertical excitations and/or responses, the vertical dynamic behavior of the restrained isolators under triaxial excitations becomes more complicated, but still has a tendency toward elastic behavior.
4. The incorporation of snubbers into the vibration isolation system can provide extra restraints. Therefore, the displacement response can be effectively reduced to prevent the restrained isolators from plastic deformation and severe damage. Since the adoption of rubber coated in snubbers can moderately mitigate pounding effect, the acceleration response performance of I/R system, in general, is not inferior to that of I/ system.
5. The recommended value for the component amplification factor  $a_p$  and the seismic design force  $F_p$  specified in ASCE 7-10 (ASCE 2010) are further examined through the seismic simulation test results. It can be concluded that  $a_p=2.5$  might be capable of representing the horizontal acceleration amplification phenomenon of a generator equipped with I/R system even though there exists obvious rocking effect. However, the seismic force demands for static design of I/R

system might not be appropriate and conservative enough.

## REFERENCES:

- American Society of Civil Engineers (ASCE). 2010. *Minimum design loads for buildings and other structures*, ASCE Standard ASCE/SEI 7-10. Virginia.
- Chen I. 2009. *Cyclic behavior of vibration isolation systems of mechanical/electrical equipment*. Master's Thesis. Department of Civil and Construction Engineering, National Taiwan University of Science and Technology.
- Eidinger J. 2007. *Fragility of non-structural components for FEMA benefit cost analysis*. California: G&E Engineering Systems Inc.
- Electric Power Research Institute (EPRI). 1991. *Summary of the seismic adequacy of twenty classes of equipment required for the safe shutdown of nuclear plants*. Technical Report NP-7149-D. California.
- Electric Power Research Institute (EPRI). 1996. *Summary of the seismic adequacy of twenty classes of equipment required for the safe shutdown of nuclear plants*. Technical Report NP-7149-DSUPPLEMEN. California.
- Fathali S, Filiatrault A. 2007a. *Experimental seismic-performance evaluation of isolation/restraint systems for mechanical equipment; Part I: Heavy equipment study*. Technical Report MCEER-07-0007. Multidisciplinary Center for Earthquake Engineering Research (MCEER), The State University of New York at Buffalo.
- Fathali S, Filiatrault A. 2007b. *Experimental seismic-performance evaluation of isolation/restraint systems for mechanical equipment; Part II: Light equipment study*. Technical Report MCEER-07-0022. Multidisciplinary Center for Earthquake Engineering Research (MCEER), The State University of New York at Buffalo.
- Federal Emergency Management Agency (FEMA). 2011. *Reducing the risks of nonstructural earthquake damage—a practical guide (FEMA E-74)*. 4th ed. Washington, D.C.
- Harmony Rubber Industry Co. Ltd. (<http://www.ys-air.com/>)
- ICC Evaluation Service, Inc. (ICC-ES). 2010. *Acceptance criteria for seismic qualification by shaking-table testing of nonstructural components and systems*, ICC-ES AC156. California.
- Lam FCF. 1985. *Analytical and experimental studies of the behavior of equipment vibration isolators under seismic condition*. Master's Thesis. Department of Civil Engineering, University of British Columbia.
- Miranda E, Mosqueda G, Retamales R, Pekcan G. 2012. Performance of nonstructural components during the 27 February 2010 Chile earthquake. *Earthq Spectra*. 28(S1): S453–71.

**Table 1 Seismic simulation test program**

Test name	$S_{DS}$	$z/h$		Nominal intensity scale factor	Excitation direction	Test PA (g)
		Horz.	Vert.			
AC156 -1F-1	0.8	0	0	10%	Triaxial X/ Y/ Z	0.04/ 0.04/ 0.02
				30%		0.11/ 0.11/ 0.07
				60%		0.18/ 0.29/ 0.13
				100%		0.37/ 0.44/ 0.32
AC156 -1F-2	0.8	0	0	10%	Triaxial X/ Y/ Z	0.03/ 0.04/ 0.02
				30%		0.11/ 0.11/ 0.07
				60%		0.18/ 0.22/ 0.14
				100%		0.34/ 0.38/ 0.27
AC156 -1F-3	0.8	0	0	10%	Triaxial X/ Y/ Z	0.04/ 0.04/ 0.03
				30%		0.17/ 0.16/ 0.09
				60%		0.29/ 0.29/ 0.19
				100%		0.53/ 0.47/ 0.31
AC156 -RF	0.6	1	0	10%	Triaxial X/ Y/ Z	0.08/ 0.06/ 0.03
				30%		0.21/ 0.20/ 0.05
				60%		0.45/ 0.40/ 0.10
				100%		0.98/ 0.84/ 0.21
				120%		1.17/ 0.99/ 0.24

**Table 2 System identification results by using sine sweep and impulse tests**

Dynamic characteristic	Test Scheme I (I/ system)	Test Scheme II (I/R system)
Fundamental modal period (Hz)	Longitudinal (X)	2.75
	Transverse (Y)	2.50
	Vertical (Z)	4.38
	Rocking along longitudinal (X) axis	2.15
	Rocking along transverse (Y) axis	2.29
Equivalent damping ratio (%)	Longitudinal (X)	2.76
	Transverse (Y)	2.72
	Vertical (Z)	1.04

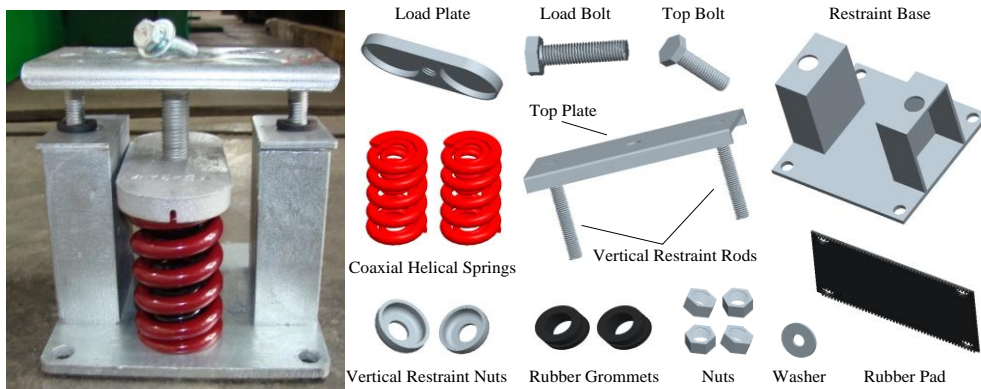


Figure 1. Detailed component illustration of tested restrained isolators

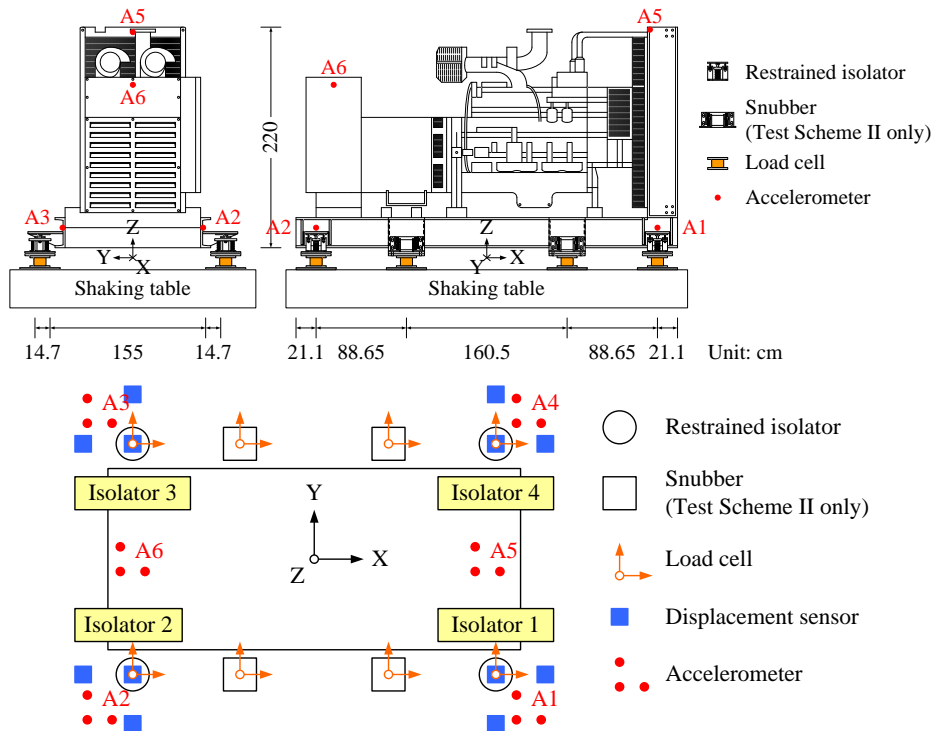


Figure 2. Test setup and measurement instrumentation layout

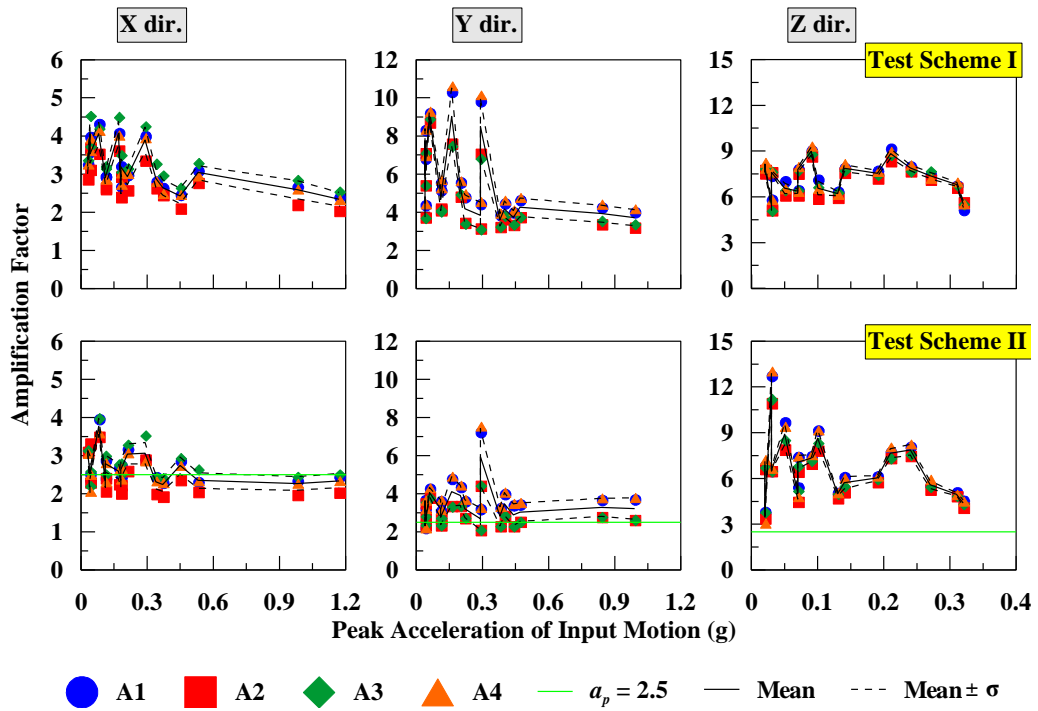


Figure 3. Acceleration transmission ratios of Test Schemes I and II under all triaxial excitations

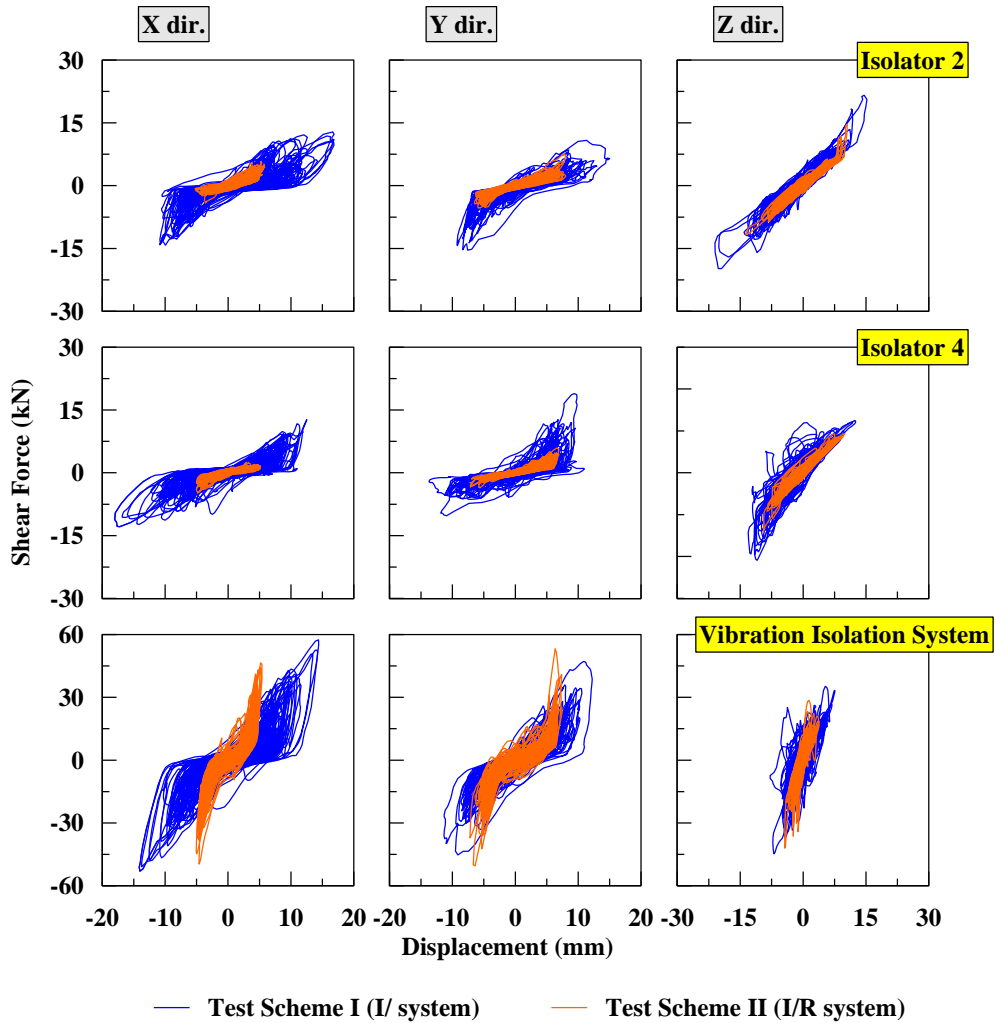


Figure 4. Hysteresis loops of Test Schemes I and II under 120% triaxial AC156-RF

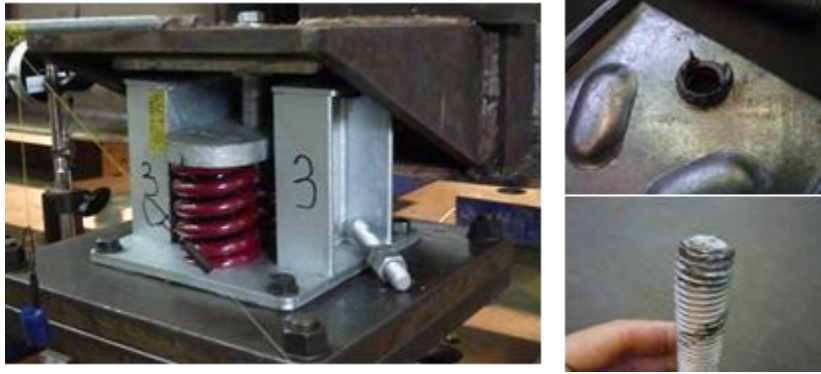


Figure 5. Failure modes of tested restrained isolators

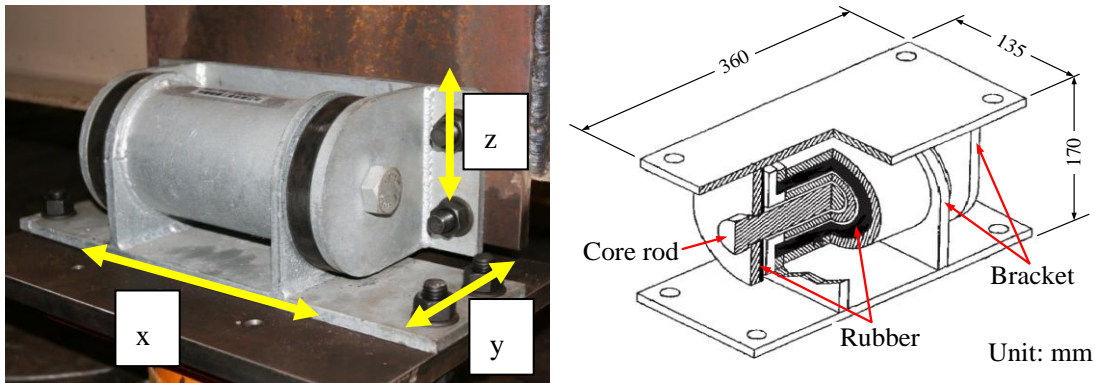


Figure 6. Detailed component illustration of tested snubbers

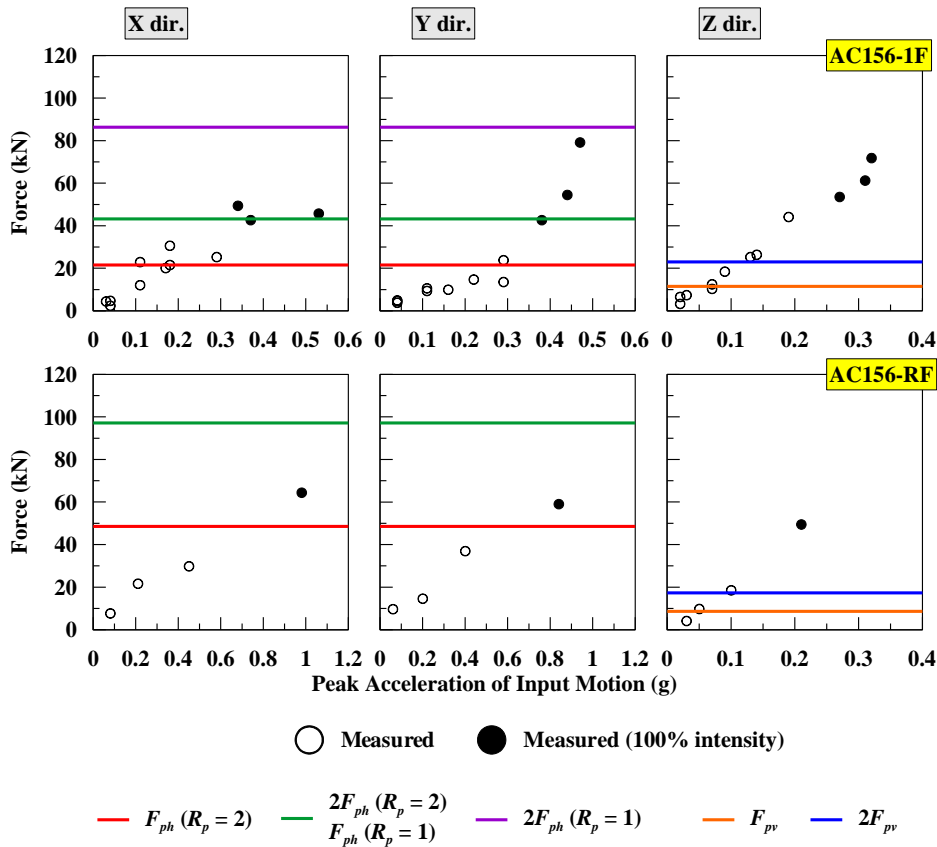


Figure 7. Maximum force responses transmitted by I/R system under all triaxial excitations